

Synthesis and Structures of Reduced Niobates with Four Perovskite-like Layers and Their Semiconducting Properties

W. Sugimoto,^{*,1} H. Ohkawa,^{*} M. Naito,^{*} Y. Sugahara,^{*,2} and K. Kuroda^{*,†}

^{*} Department of Applied Chemistry, School of Science and Engineering, Waseda University, Ohkubo-3, Shinjuku-ku, Tokyo 169-8555, Japan; and

[†] Kagami Memorial Laboratory for Materials Science and Technology, Waseda University, Nishiwaseda-2, Shinjuku-ku, Tokyo 169-0051, Japan

Received March 29, 1999; in revised form July 27, 1999; accepted August 27, 1999

Carriers were successfully doped into $\text{RbCa}_2\text{NaNb}_4\text{O}_{13}$ by the substitution of Sr^{2+} for Na^+ , yielding electroconducting niobates with a layered structure consisting of four perovskite-like layers. Single-phase products of polycrystalline $\text{RbCa}_2\text{Na}_{1-x}\text{Sr}_x\text{Nb}_4\text{O}_{13}$ ($x = 0.2$ and 0.4) were synthesized by the solid-state reaction of $\text{RbCa}_2\text{Nb}_3\text{O}_{10}$, $\text{Sr}_5\text{Nb}_4\text{O}_{15}$, Nb_2O_5 , and Nb metal. The solid solutions were indexed based on a tetragonal structure, corresponding to the end-member $\text{RbCa}_2\text{NaNb}_4\text{O}_{13}$. With the increase in the amount of strontium substitution, an expansion of the c -axis was observed while the a -axis was essentially constant. The products showed semiconducting properties.

© 1999 Academic Press

Key Words: niobate; solid-state reaction; layered perovskite; reduced oxidation state; Rietveld analysis; electrical conduction.

1. INTRODUCTION

A large class of transition metal oxides possess structures consisting of two-dimensionally stacked perovskite-like slabs: $A_{n+1}B_nO_{3n+1}$ (1), $\text{Bi}_2A_{n-1}B_nO_{3n+3}$ (2), and $MA_{n-1}B_nO_{3n+1}$ are well-known examples (3, 4). These structures are ideal for relating the thickness of the perovskite-like slabs n with the properties. For example, the change in the electrical properties of $(\text{La}, \text{Sr})_{n+1}\text{Mn}_n\text{O}_{3n+1}$ ($n = 1, 2, 3$, and ∞) (5), $\text{Sr}_{n+1}\text{V}_n\text{O}_{3n+1}$ ($n = 1, 2$, and ∞) (6, 7), $\text{La}_{n+1}\text{Ni}_n\text{O}_{3n+1}$ ($n = 1, 2, 3$, and ∞) (8), and $(\text{Sr}_{0.95}, \text{La}_{0.05})_{n+1}\text{Ti}_n\text{O}_{3n+1-\delta}$ ($n = 1$ and 2) (9) has been discussed based on the difference in the thickness of the perovskite-like slabs.

Recently, the incorporation of conducting electrons into niobates with a layered-perovskite structure, $M[A_{n-1}\text{Nb}_n\text{O}_{3n+1}]$, has drawn attention. The structure of $M[A_{n-1}\text{Nb}_n\text{O}_{3n+1}]$ consists of n perovskite-like layers with

a monovalent cation M occupying the interlayer space. The reduced niobates for the $n = 2$ and 3 compounds have been synthesized by chemical or electrochemical intercalation of excess ions (H^+ , Li^+ , and Rb^+) into the interlayer (9–17) and by cation substitution by solid-state reaction (18, 19). Most of the early studies have emphasized the structural characterization of the reduced products.

The electrical properties of carrier-doped $n = 2$ and 3 members have been reported recently. We have reported the synthesis and electrical properties of the $n = 3$ member $\text{KCa}_{2-x}\text{Ln}_x\text{Nb}_3\text{O}_{10}$ ($\text{Ln} = \text{La}, \text{Ce}, \text{Nd}, \text{Sm}$, and Gd) (18, 19). The observed $(\log \rho) \propto T$ dependence was interpreted based on a model assuming tunneling conduction through vibrating barriers, and the structure–property relation was established (18, 19). Recently, it has been reported that the $n = 3$ member $\text{Li}_x\text{KCa}_2\text{Nb}_3\text{O}_{10}$ shows a superconducting transition below 6 K (15–17), whereas the $n = 2$ member $\text{Li}_x\text{KLaNb}_2\text{O}_7$ shows no superconducting transition down to 0.5 K (15). This suggests that the thickness of the perovskite-like slabs influences the superconducting properties in $M[A_{n-1}\text{Nb}_n\text{O}_{3n+1}]$.

The synthesis and structural characterization of the $n = 4$ member, $\text{RbCa}_2\text{NaNb}_4\text{O}_{13}$, have been reported (4, 20). The schematic structure of $\text{RbCa}_2\text{NaNb}_4\text{O}_{13}$ is shown in Fig. 1. In light of the variation in the electrical properties as a function of n in the two-dimensional perovskites reported so far, the electrical properties of higher n members of $M[A_{n-1}\text{Nb}_n\text{O}_{3n+1}]$ are of interest. Here, we report the doping of carriers into the $n = 4$ member of the layered perovskite $\text{RbCa}_2\text{NaNb}_4\text{O}_{13}$ by the substitution of Sr^{2+} for Na^+ and their structures and electrical properties.

2. EXPERIMENTAL

$\text{RbCa}_2\text{Nb}_3\text{O}_{10}$, $\text{Sr}_5\text{Nb}_4\text{O}_{15}$, and NaNbO_3 were prepared by the solid-state reactions of appropriate amounts of Rb_2CO_3 , CaCO_3 , SrCO_3 , Na_2CO_3 , and Nb_2O_5 under ambient atmosphere. A 50% excess amount of Rb_2CO_3 was used in the case of $\text{RbCa}_2\text{Nb}_3\text{O}_{10}$. The product was washed

¹ Current address: Department of Fine Materials Engineering, Faculty of Textile Science and Technology, Shinshu University, 3-15-1 Tokida, Ueda 386-8567, Japan.

² To whom correspondence should be addressed. E-mail: ys6546@mn.waseda.ac.jp.

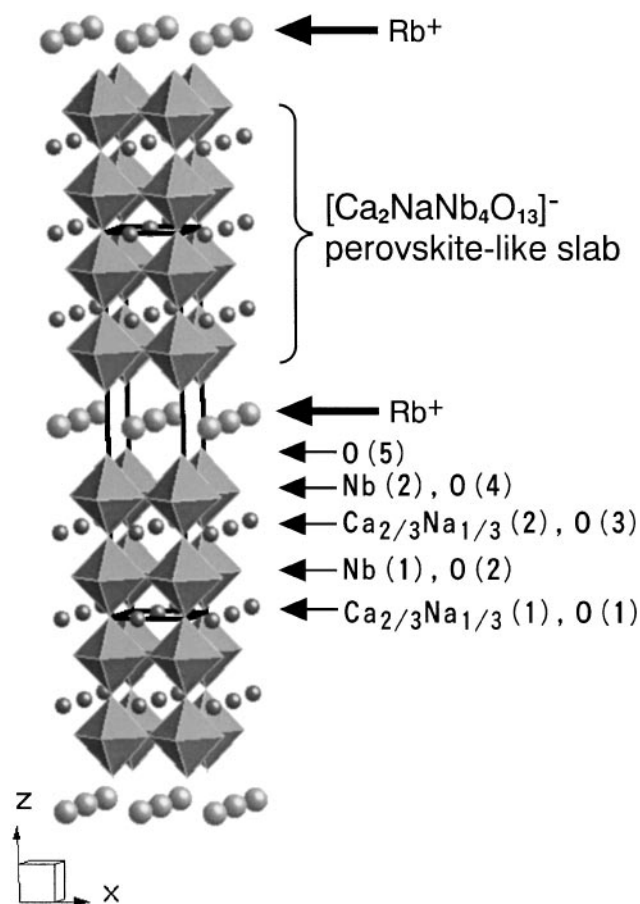
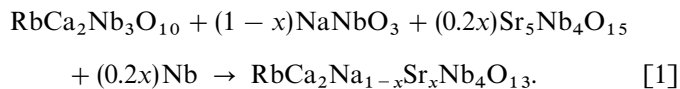


FIG. 1. Schematic crystal structure of $\text{RbCa}_2\text{NaNb}_4\text{O}_{13}$.

with deionized water after completion of the reaction. X-ray diffraction (XRD) (Mac Science MXP³ diffractometer with monochromated $\text{CuK}\alpha$ radiation) of the above oxides indicated single-phase formation, and inductively coupled plasma emission spectroscopy (ICP) (Nippon Jarrell Ash, ICAP575 MarkII) showed that the cation ratios were consistent with the nominal ones.

Polycrystalline samples with nominal compositions of $\text{RbCa}_2\text{Na}_{1-x}\text{Sr}_x\text{Nb}_4\text{O}_{13}$ ($x = 0.2, 0.4, \text{ and } 0.5$) were synthesized from $\text{RbCa}_2\text{Nb}_3\text{O}_{10}$, NaNbO_3 , $\text{Sr}_5\text{Nb}_4\text{O}_{15}$, and Nb according to the following equation:



All of the starting oxides were dried for at least 1 day at 100°C before use. The end-member $\text{RbCa}_2\text{NaNb}_4\text{O}_{13}$ was synthesized by the solid-state reactions of $\text{RbCa}_2\text{Nb}_3\text{O}_{10}$ and NaNbO_3 at 1200°C for 3 h in air (20). After thorough grinding, the reagents were pressed and placed in an alumina boat surrounded by powders having the same

composition to prevent contamination. The reactor tube was evacuated to $\sim 8.5 \times 10^{-3}$ Pa before argon purging and Ti powder was placed in the reactor tube as an oxygen getter to minimize oxidation during the synthesis. The reagents were fired at 1200°C for several hours, with intermittent grinding after every 3 h of firing. The firing sequence was repeated twice.

The morphology of the products was studied with a scanning electron microscope (SEM) (Hitachi, S-2500). Crystalline phases were identified by XRD. Structural parameters were determined by the Rietveld analysis program RIETAN (21, 22). The cation ratios were determined by ICP analysis. For the ICP measurements, the samples were decomposed in a mixture of HF , HCl , and HNO_3 by heating at 200°C for at least 3 h. Resistivity data were collected from 80 to 280 K using a standard dc four-probe method.

3. RESULTS AND DISCUSSION

Table 1 summarizes the compositional analysis results of the products obtained as single phases. The cation ratios were in agreement with the nominal composition for all x . Thus, the discussion herein is based on the assumption that the substitution of Sr^{2+} for Na^+ produces an equimolar amount of Nb^{4+} during the synthesis.

The XRD patterns of the products are shown in Fig. 2. Preferred orientation was observed along the $[00l]$ plane, consistent with the plate-like morphology of the samples observed in the scanning electron micrographs. The XRD

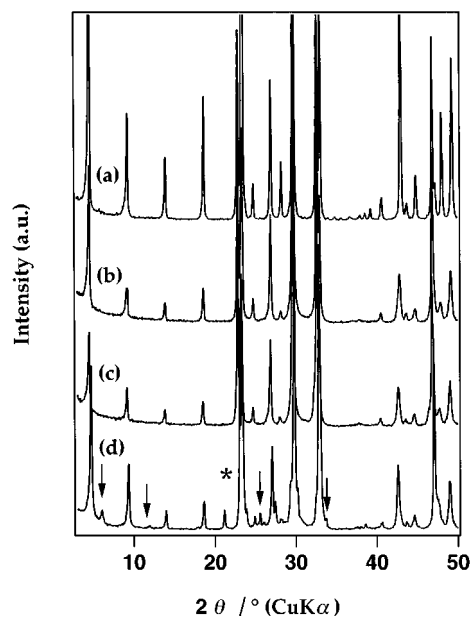


FIG. 2. XRD patterns of $\text{RbCa}_2\text{Na}_{1-x}\text{Sr}_x\text{Nb}_4\text{O}_{13}$ with (a) $x = 0$, (b) $x = 0.2$, (c) $x = 0.4$, and (d) $x = 0.5$. Arrows in (d) represent peaks due to the $n = 3$ compound. The peak with an asterisk in (d) is an unidentified peak.

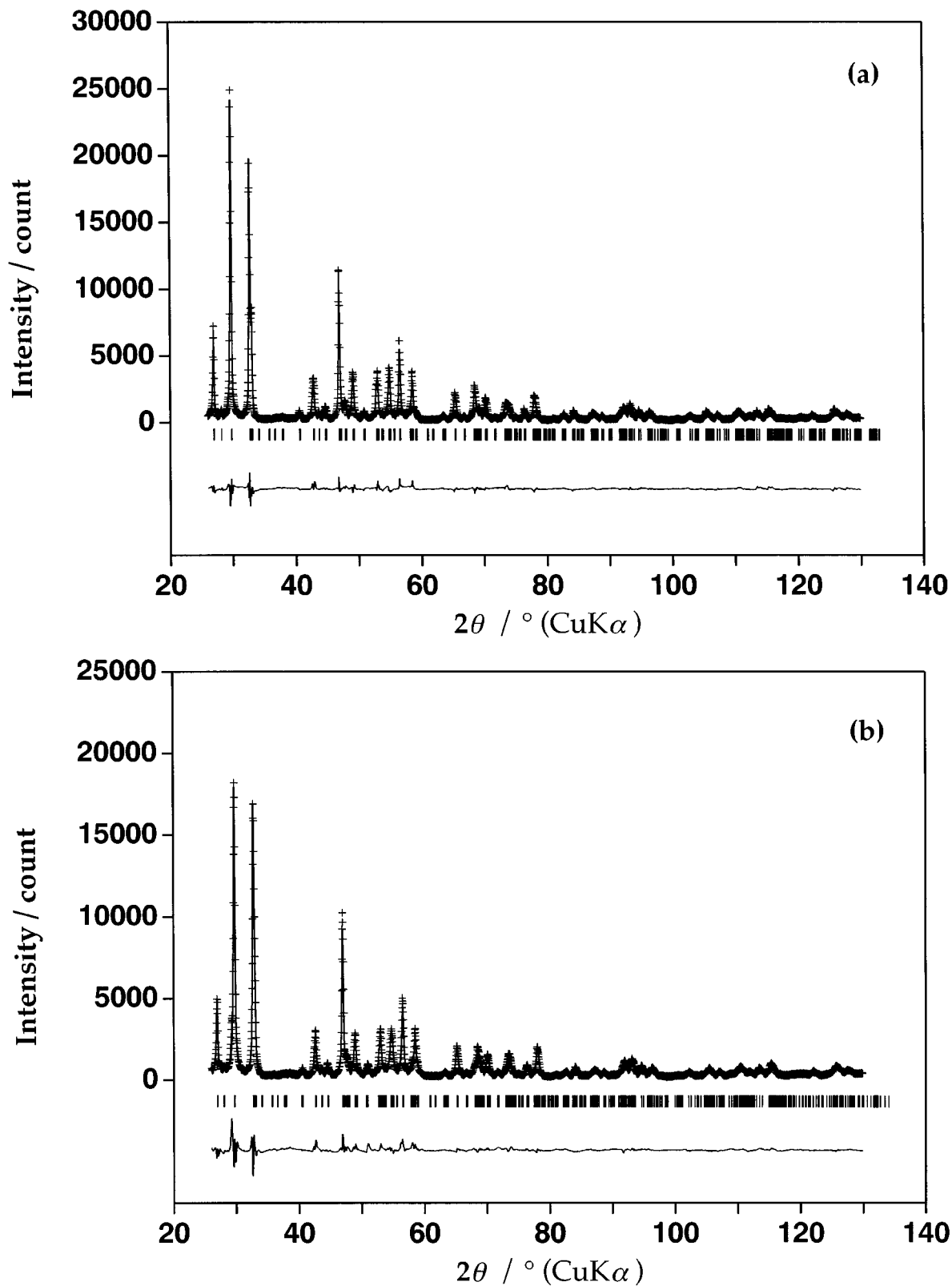


FIG. 3. XRD pattern fittings for (a) $\text{RbCa}_2\text{Na}_{0.8}\text{Sr}_{0.2}\text{Nb}_4\text{O}_{13}$ and (b) $\text{RbCa}_2\text{Na}_{0.6}\text{Sr}_{0.4}\text{Nb}_4\text{O}_{13}$. The observed (crosses) and calculated (solid line) patterns are shown in the top traces. The vertical lines in the middle represent the positions of the possible Bragg reflections. The lower curves are the difference between the observed and calculated intensities.

TABLE 1
Composition of the Products

x	Composition ^{a,b}
0	Rb _{1.00} Ca _{2.06} Na _{1.06} Nb ₄ O ₁₃
0.2	Rb _{1.00} Ca _{2.00} Na _{0.80} Sr _{0.21} Nb ₄ O ₁₃
0.4	Rb _{1.04} Ca _{2.07} Na _{0.61} Sr _{0.40} Nb ₄ O ₁₃

^a Compositions were normalized by setting the amount of niobium to 4.

^b Amount of oxygen was set to 13.

pattern for $x = 0$ was indexed based on a primitive-tetragonal cell, in agreement with a previous report (20). Single-phase RbCa₂Na_{1-x}Sr_xNb₄O₁₃ was obtained for $x = 0.2$ and 0.4 with repeated firings. No extra reflections for $x = 0.2$ and 0.4 were evident in the XRD patterns when compared to that of $x = 0$, and all the diffraction peaks were indexed based on a primitive-tetragonal cell. When $x = 0.5$, an unidentified peak at $2\theta = 21.16^\circ$ and weak diffraction peaks due to RbCa₂Nb₃O₁₀ were observed besides the intended phase. A single phase for $x = 0.5$ could not be obtained even with repeated firings or firing at higher temperature. Thus, the solubility limit is between $x = 0.4$ and 0.5 under the present synthetic conditions.

The structure of the $x = 0$ compound was refined by Rietveld analysis assuming a random distribution of Ca and Na at the A site (20). The crystallographic data corresponded to those of a previous report (20). Since the indexing of the XRD patterns for $x = 0.2$ and 0.4 indicated the preservation of the symmetry with substitution. Rietveld analysis for these compounds was conducted with the same space group as that for $x = 0$. A random distribution of the A -site cations (Ca, Na, and Sr) was also assumed. The outputs from the Rietveld refinement are shown in Fig. 3, and the crystallographic data are given in Table 2. The a -axis was

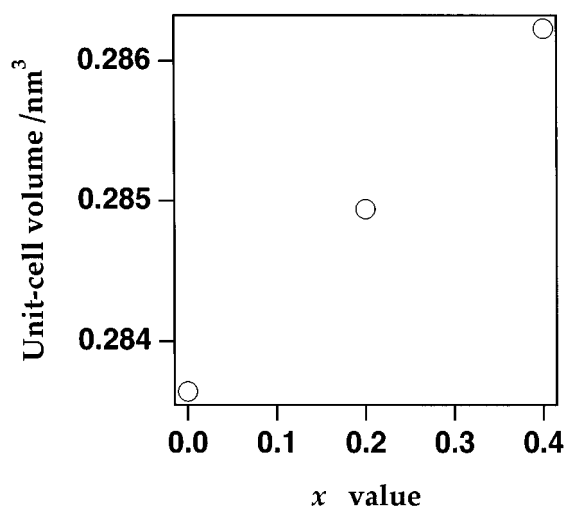


FIG. 4. Evolution of the unit-cell volume as a function of x .

TABLE 2
Crystallographic data for RbCa₂NaNb₄O₁₃, RbCa₂Na_{0.8}Sr_{0.2}Nb₄O₁₃, and RbCa₂Na_{0.6}Sr_{0.4}Nb₄O₁₃^a

Sample	Atom	Position	x	y	z	B (nm ²) ^c	
RbCa ₂ NaNb ₄ O ₁₃	Rb	1d	0.5	0.5	0.5	0.028(3)	
	A(1) ^b	1c	0.5	0.5	0	0.010(2)	
	$a = 0.38727(1)$ nm	A(2) ^b	2h	0.5	0.5	0.2240(7)	0.010
	$c = 1.89116(6)$ nm	Nb(1)	2g	0	0	0.1057(2)	0.0028(9)
		Nb(2)	2g	0	0	0.3293(2)	0.0028
	$R_{wp} = 0.1299$	O(1)	1a	0	0	0	0.036(4)
	$R_p = 0.0969$	O(2)	4i	0	0.5	0.101(1)	0.036
	$R_e = 0.0340$	O(3)	2g	0	0	0.205(2)	0.036
	$R_I = 0.0349$	O(4)	4i	0	0	0.309(1)	0.036
	$R_F = 0.0217$	O(5)	2g	0	0	0.420(2)	0.036
RbCa ₂ Na _{0.8} Sr _{0.2} Nb ₄ O ₁₃	Rb	1d	0.5	0.5	0.5	0.048(4)	
	A(1) ^b	1c	0.5	0.5	0	0.012(1)	
	$a = 0.38716(1)$ nm	A(2) ^b	2h	0.5	0.5	0.2248(7)	0.010
	$c = 1.90092(8)$ nm	Nb(1)	2g	0	0	0.1054(3)	0.0030(8)
		Nb(2)	2g	0	0	0.3289(3)	0.0030
	$R_{wp} = 0.0990$	O(1)	1a	0	0	0	0.037(3)
	$R_p = 0.0769$	O(2)	4i	0	0.5	0.104(2)	0.037
	$R_e = 0.0355$	O(3)	2g	0	0	0.214(2)	0.037
	$R_I = 0.0339$	O(4)	4i	0	0	0.308(1)	0.037
	$R_F = 0.0221$	O(5)	2g	0	0	0.416(2)	0.037
RbCa ₂ Na _{0.6} Sr _{0.4} Nb ₄ O ₁₃	Rb	1d	0.5	0.5	0.5	0.044(5)	
	A(1) ^b	1c	0.5	0.5	0	0.008(2)	
	$a = 0.38704(3)$ nm	A(2) ^b	2h	0.5	0.5	0.2236(9)	0.008
	$c = 1.9107(1)$ nm	Nb(1)	2g	0	0	0.1056(5)	0.006(10)
		Nb(2)	2g	0	0	0.3285(4)	0.006
	$R_{wp} = 0.1216$	O(1)	1a	0	0	0	0.034(5)
	$R_p = 0.0881$	O(2)	4i	0	0.5	0.101(3)	0.034
	$R_e = 0.0359$	O(3)	2g	0	0	0.215(3)	0.034
	$R_I = 0.0426$	O(4)	4i	0	0	0.309(2)	0.034
	$R_F = 0.0243$	O(5)	2g	0	0	0.421(3)	0.034

^a Space group $P4/mmm$; No. 123. 2θ step size = 0.04, total number of reflections = ca. 400, number of profile points = 2601. Number in parentheses represents estimated standard deviation. Values without standard deviation were constrained. The occupation factor was set to unity for all positions.

^b The cation ratios in $A(1)$ and $A(2)$ were confined to Ca:Na = 2/3:1/3 for RbCa₂NaNb₄O₁₃, Ca:Na:Sr = 2/3:4/15:1/15 for RbCa₂Na_{0.8}Sr_{0.2}Nb₄O₁₃, and Ca:Na:Sr = 2/3:3/15:2/15 for RbCa₂Na_{0.6}Sr_{0.4}Nb₄O₁₃.

^c The isotropic atomic displacement parameters for the same cation species were constrained to be equal.

essentially unchanged, while the c -axis increased linearly, resulting in an overall increase in the unit-cell volume (Fig. 4). The increase is attributed to the larger ionic radii of Sr²⁺ (0.144 nm) and Nb⁴⁺ (0.068 nm) compared to Na⁺ (0.139 nm) and Nb⁵⁺ (0.064 nm) (23).

Calculation of the bond distances showed that the Nb–O bond extending toward the interlayer had the shortest distance (Nb(2)–O(5) = 0.177(6) nm). The longest Nb–O bond was Nb(2)–O(3) = 0.216(7) nm. The inner two perovskite-like slabs are closer to an ideal octahedron than the outer ones, as was the case for $x = 0$ (20). No drastic change in the

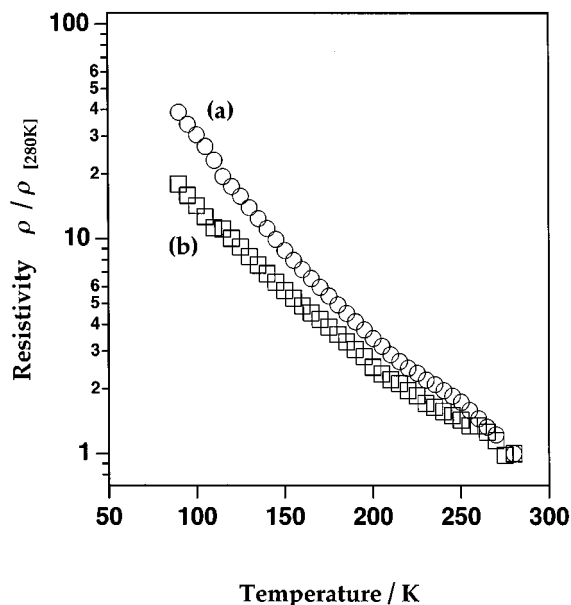


FIG. 5. Temperature dependence of the normalized resistivity for (a) $\text{RbCa}_2\text{Na}_{0.8}\text{Sr}_{0.2}\text{Nb}_4\text{O}_{13}$ and (b) $\text{RbCa}_2\text{Na}_{0.6}\text{Sr}_{0.4}\text{Nb}_4\text{O}_{13}$.

crystallographic environments of the inner and outer two perovskite-like slabs upon doping was apparent.

The temperature dependence of the normalized resistivity on a logarithmic scale is shown in Fig. 5. The samples showed semiconducting behavior, with typical resistivity at room temperature in the order of 10^1 – 10^2 Ω m. The resistivity for $\text{RbCa}_2\text{Na}_{0.6}\text{Sr}_{0.4}\text{Nb}_4\text{O}_{13}$ was slightly less temperature-dependent than that of $\text{RbCa}_2\text{Na}_{0.8}\text{Sr}_{0.2}\text{Nb}_4\text{O}_{13}$. Since a linear relation could not be obtained in the $(\log \rho)$ vs T^{-1} plot in the temperature region $80 \leq T \leq 280$, the thermally activated electron-hopping conduction mechanism could not be applied. In the case of $\text{Na}_{1-x}\text{Sr}_x\text{NbO}_3$ ($0.2 \leq x \leq 0.4$) (24) and $\text{KCa}_{2-x}\text{La}_x\text{Nb}_3\text{O}_{10}$ ($0.1 \leq x \leq 0.3$) (18), a linear $(\log \rho) \propto T$ relation was observed in the temperature region $80 \leq T \leq 280$. The electrical properties in these compounds were interpreted based on the tunneling conduction of small polarons through vibrating barriers (25). The general shape of the $(\log \rho)$ vs T plot (Fig. 5) suggests that the resistivity behavior of $\text{RbCa}_2\text{Na}_{1-x}\text{Sr}_x\text{Nb}_4\text{O}_{13}$ may also be explained by the tunneling conduction of small polarons through vibrating barriers (25). However, since the linearity was not preserved throughout the whole temperature region studied ($80 \leq T \leq 280$), other conduction mechanisms should also contribute to the electrical properties. A deviation from the apparent $(\log \rho) \propto T$ behavior was also observed for $\text{Na}_{1-x}\text{Sr}_x\text{NbO}_3$ ($x = 0.10$ and 0.15) when the Sr content was small (24).

4. CONCLUSIONS

Polycrystalline samples of reduced niobates possessing a four-layered perovskite structure, $\text{RbCa}_2\text{Na}_{1-x}\text{Sr}_x\text{Nb}_4$

O_{13} ($x = 0.2$ and 0.4), were synthesized and their structures and electrical properties were studied. The tetragonal structure of the end member $\text{RbCa}_2\text{NaNb}_4\text{O}_{13}$ was retained with the substitution. The a -axis was essentially constant, while the c -axis increased linearly with an increase in x . Semiconducting properties were obtained for both $x = 0.2$ and $x = 0.4$.

ACKNOWLEDGMENTS

Y.S. thanks the Advanced Research Center for Science and Engineering at Waseda University for financial support as Individual Research. This work was financially supported in part by a Grant-in-Aid for JSPS Fellows (5727) from the Ministry of Education, Science, Sports, and Culture, Japan.

REFERENCES

1. (a) S. N. Ruddlesden and P. Popper, *Acta Crystallogr.* **10**, 538 (1957). (b) S. N. Ruddlesden and P. Popper, *Acta Crystallogr.* **11**, 54 (1958).
2. (a) B. Aurivillius, *Ark. Kemi.* **1**, 463 (1949). (b) B. Aurivillius, *Ark. Kemi.* **1**, 499 (1949). (c) B. Aurivillius, *Ark. Kemi.* **2**, 519 (1950).
3. M. Dion, M. Ganne, and M. Tournoux, *Mater. Res. Bull.* **16**, 1429 (1981).
4. M. Dion, M. Ganne, and M. Tournoux, *Rev. Chim. Miner.* **23**, 61 (1986).
5. R. A. Mohan Ram, P. Ganguly, and C. N. R. Rao, *J. Solid State Chem.* **70**, 82 (1987).
6. A. Nozaki, H. Yoshikawa, T. Wada, H. Yamauchi, and S. Tanaka, *Phys. Rev. B* **43**, 181 (1991).
7. M. Itoh, M. Shikano, H. Kawaji, and T. Nakamura, *Solid State Commun.* **80**, 545 (1991).
8. R. A. Mohan Ram, L. Ganapathi, P. Ganguly, and C. N. R. Rao, *J. Solid State Chem.* **63**, 139 (1986).
9. R. Jones and W. R. McKinnon, *Solid State Ionics* **45**, 173 (1991).
10. P. Gomez-Romero, M. R. Palacin, N. Casan, and A. Fuertes, *Solid State Ionics* **63–65**, 424 (1993).
11. M. Sato, T. Jin, and H. Ueda, *Chem. Lett.* **1994**, 161 (1994).
12. A. R. Armstrong and P. A. Anderson, *Inorg. Chem.* **33**, 4366 (1994).
13. M. R. Palacin, M. Lira, J. L. Garcia, M. T. Caldes, N. Casan-Pastor, A. Fuertes, and P. Gomez-Romero, *Mater. Res. Bull.* **31**, 217 (1996).
14. C. Bohnke, O. Bohnke, and J. L. Fourquet, *J. Electrochem. Soc.* **144**, 1151 (1997).
15. Y. Takano, S. Takayanagi, S. Ogawa, T. Yamadaya, and N. Mori, *Solid State Commun.* **103**, 215 (1997).
16. H. Fukuoka, T. Isami, and S. Yamanaka, *Chem. Lett.* **1997**, 703 (1997).
17. Y. Takano, H. Taketomi, H. Tsurumi, T. Yamadaya, and N. Mori, *Physica B* **237–238**, 68 (1997).
18. D. Hamada, M. Machida, Y. Sugahara, and K. Kuroda, *J. Mater. Chem.* **6**, 69 (1996).
19. D. Hamada, W. Sugimoto, Y. Sugahara, and K. Kuroda, *J. Ceram. Soc. Jpn.* **105**, 284 (1997).
20. M. Sato, Y. Kono, and T. Jin, *J. Ceram. Soc. Jpn.* **101**, 980 (1993).
21. F. Izumi, in "The Rietveld Method," p. 236. Oxford Univ. Press, London, 1993.
22. Y. I. Kim and F. Izumi, *J. Ceram. Soc. Jpn.* **102**, 401 (1994).
23. R. D. Shannon, *Acta Crystallogr., Sect. A* **32**, 751 (1976).
24. B. Ellis, J. P. Doumerc, P. Dordor, M. Pouchard, and P. Hagenmuller, *Solid State Commun.* **51**, 913 (1984).
25. C. M. Hurd, *J. Phys. C* **18**, 6487 (1985).